

Continuous-Flow O-Alkylation of Biobased Derivatives with Dialkyl Carbonates in the Presence of Magnesium–Aluminium Hydrotalcites as Catalyst Precursors

Lisa Cattelan,^[a, b] Alvisè Perosa,^[a] Piero Riello,^[a] Thomas Maschmeyer,^[b] and Maurizio Selva^{*[a]}

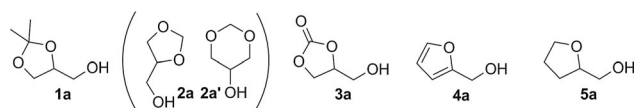
The base-catalysed reactions of OH-bearing biobased derivatives (BBDs) including glycerol formal, solketal, glycerol carbonate, furfuryl alcohol and tetrahydrofurfuryl alcohol with non-toxic dialkyl carbonates (dimethyl and diethyl carbonate) were explored under continuous-flow (CF) conditions in the presence of three Na-exchanged Y- and X-faujasites (FAUs) and four Mg–Al hydrotalcites (HTs). Compared to previous etherification protocols mediated by dialkyl carbonates, the reported procedure offers substantial improvements not only in terms

of (chemo)selectivity but also for the recyclability of the catalysts, workup, ease of product purification and, importantly, process intensification. Characterisation studies proved that both HT30 and KW2000 hydrotalcites acted as catalyst precursors: during the thermal activation pre-treatments, the typical lamellar structure of the hydrotalcite was broken down gradually into a MgO-like phase (periclase) or rather a magnesia–alumina solid solution, which was the genuine catalytic phase.

Introduction

In the past 15 years, an enormous effort has been devoted to the identification of the most promising biomass-derived compounds. Among the available analyses, extensive work performed by the US Department of Energy in 2004 and its revision in 2010 still represent cornerstones in this field. For the first time, they offered rational criteria for the selection of the so-called “top 10” platform chemicals, that is, a small group of biobased derivatives (BBDs) that could be utilised as building blocks for higher-value products and materials.^[1] Although this approach has been refined further over the years,^[2] current top 10 lists of biomass-derived platform compounds still include most of the originally identified compounds, particularly mono- and dicarboxylic-functionalised acids, 3-hydroxybutyrolactone, several bio-hydrocarbons derived from isoprene, glycerol and derivatives as well as several other sugars such as sorbitol and xylitol. These considerations have inspired us to try to integrate green protocols mediated by dialkyl carbonates (ROCO₂R, DAICs)^[3] with the chemical valorisation of biobased platform molecules. Such an activity requires a multidisciplinary approach to combine aspects of organic and physical chemistry as well as chemical engineering and materials science.

Within this context, our attention has been focused on five model OH-bearing BBDs (Scheme 1) including solketal (**1 a**), glycerol formal (**2 a/2 a'**) and glycerol carbonate (**3 a**), which are among the most celebrated derivatives of glycerol. The appli-



Scheme 1. Model OH-bearing BBDs.

cations of these compounds span multiple sectors from fine chemicals, cosmetics and pharmaceuticals to biofuels and lubricants, biobased solvents and polymers.^[4] The availability of glycerol is mostly fuelled by plant-oil-based biodiesel manufacture, which generates large amounts of glycerol as a co-product.^[5] The other two compounds shown in Scheme 1, that is, furfuryl alcohol (**4 a**) and its hydrogenated homologue tetrahydrofurfuryl alcohol (**5 a**), are derived from furfural, which, in turn, is generated through the dehydration of the sugar components (glucose and xylose) that constitute a large portion of lignocellulosic biomass.^[6] Compounds **4 a** and **5 a** find uses as modifiers and templates for polymers, as fibers and nanocomposites^[7] and as sources of polyols.^[8]

In addition, the presence of an OH-capped tether (hydroxymethylene group) enables an avenue for the derivatisation of all five compounds (**1 a–5 a**): of particular note, esterification and alkylation protocols allow for the expansion of the potential of OH-BBDs through the synthesis of substantially value-added products, including intermediates, solvents and biologically active molecules such as glycerol ethers, esters and carbo-

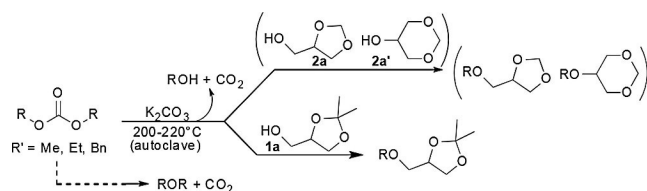
[a] L. Cattelan, Prof. A. Perosa, Prof. P. Riello, Prof. M. Selva
Department of Molecular Sciences and Nanosystems
Università Ca' Foscari Venezia
Via Torino, 155, Venezia Mestre (Italy)
E-mail: selva@unive.it

[b] L. Cattelan, Prof. T. Maschmeyer
Laboratory of Advanced Catalysis for Sustainability
School of Chemistry F11
University of Sydney
Sydney, 2006 (Australia)

Supporting Information and the ORCID identification number(s) for the author(s) of this article can be found under <http://dx.doi.org/10.1002/cssc.201601765>.

nates^[9] as well as additives for biodiesel blends based on furanyl ether derivatives.^[6a]

The combined effect of a high reaction temperature (200–220 °C) and a base catalyst (K₂CO₃) allowed an almost exclusive *O*-alkylation of glycerol acetals (GAs). The reaction showed excellent features from both synthetic and environmental standpoints because it not only proceeded with etherification selectivities and yields as high as 99 and >80%, respectively but also coupled the use of renewable and non-toxic reactants such as glycerol acetals and DAICs in a catalytic process with no byproducts other than CO₂ (which did not present a disposal problem) and alcohols, which were recyclable for the synthesis of dialkyl carbonates. Only trace amounts of byproducts from competitive transesterification processes were detected. However, under the explored batch conditions, the sequence suffered from two major drawbacks: 1) slow alkylation kinetics, that is, the reactions could require up to 80 h for completion, and 2) extensive competitive decarboxylations of dialkyl carbonates to form the corresponding dialkyl ethers (Scheme 2, dashed path).^[10]



Scheme 2. The etherification of glycerol acetals with dialkyl carbonates in the presence of K₂CO₃ catalyst (top). The dashed path shows the concurrent decarboxylation reaction of dialkyl carbonates.

This necessitates the use of a large excess of the alkylating agent and, importantly, involves the co-generation of an autogenous pressure of ≥ 60 bar; both of these aspects hindered the scale-up of the process. However, the benefits and disadvantages stimulated us to devise a new broad-based protocol to expand the alkylating capabilities of dialkyl carbonates to different OH-bearing BBDs and, at the same time, minimise the limitations described above. The implementation of a continuous-flow (CF) procedure was an attractive option to reach the conversion target because it offered the best possible control of the reaction parameters (*T*, *p* and reactant molar ratio) to improve the process kinetics, productivity and safety. However, under CF conditions, alkaline carbonates needed anion activators (polyethylene glycols), specifically shaped reactors (e.g., continuous-stirred-tank-reactors, CSTRs) or both to perform as catalysts,^[11] because the basicities of the alkaline carbonates were too low and they were partially soluble in the reactant DAICs and the co-produced alcohols (Scheme 2).^[12] Therefore, alternative solid systems had to be considered. Candidates were chosen from the families of faujasite (FAU) and Mg–Al hydrotalcite (HT) solids. We have reported both Y- and X-type FAUs extensively as catalysts for DAIC-promoted *N*-, *O*- and *S*-alkylations of a large variety of nucleophiles, including anilines, benzyl alcohols, aminophenols, aminobenzyl alcohols, mercaptophenols, mercaptobenzoic acids, hydroxybenzoic acids and

functionalised phenols of the lignin scaffold.^[13] However, HTs have been investigated almost exclusively as catalysts for transesterifications with dialkyl carbonates,^[14] whereas only a few reports have described the methylation of some phenols and benzyl alcohol with dimethyl carbonate over Mg–Al hydrotalcites or modified HT systems.^[15] The role of the catalyst is still under debate.

The present work demonstrates that the use of HTs allows for the setup of a particularly robust catalytic CF method for the etherification of OH-bearing BBDs with DAICs. For example, at 210 °C and ambient pressure, the model reaction of solketal (1a) with dimethyl carbonate shows the formation of the corresponding methyl ether with quantitative conversion and >99% selectivity in the presence of calcined HT Pural® MG30 (cHT30; Mg/Al=0.5) as a catalyst.

The CF protocol can be extended to the reactions of the substrates shown in Scheme 1 with both dimethyl and diethyl carbonate. Quantitative conversions and *O*-alkylation selectivity comparable to those of solketal were achieved over calcined HT catalysts, except for furfuryl alcohol (4a) for which only the transesterification derivative [(furan-2-yl)methyl methyl carbonate] was obtained. Overall, the CF procedure not only exemplifies an original approach to the upgrade of OH-bearing bio-based substrates but can also overcome the safety and scale-up limitations of batchwise reactions as it operates at atmospheric pressure and with a productivity [≈ 2 g/(g_{cat}h)] for ether derivatives that is up to 200-fold higher than those of batch methods.

Results and Discussion

The apparatus used for the CF reactions comprised an HPLC pump, an oven containing a tubular reactor filled with the catalyst, a Rheodyne sampling valve and a back-pressure regulator (the details are reported in the Supporting Information). The dialkyl carbonates including dimethyl and diethyl carbonate as well as 1a–5a were commercially available ACS-grade compounds.

Catalyst

Three alkali-metal-exchanged X- and Y-type FAUs including two commercially available NaX and NaY solids and a CsY zeolite were used. The latter was prepared as described in the Experimental Section. Four HTs were also used. Three of them were obtained from Sasol, Italy and labelled as HT30, HT63 and HT70. A fourth sample from Kyowa Kagaku Kogyo Company Limited was labelled as KW2000. Some features of these HT solids are summarised in Table 1. For KW2000, inductively coupled plasma mass spectrometry (ICP-MS) analysis was used to determine the post-synthesis Na and K residues (see Experimental Section). MgO and a 30:70 physical mixture of MgO (Aldrich, particle size 325 mesh, surface area 114 m²g⁻¹, average pore diameter 9.4 nm) and basic γ -Al₂O₃ (Macherey–Nagel, pH 9.5 \pm 0.3, particle size 50–200 μ m, surface area 130 m²g⁻¹) were also used as additional catalysts for two comparative tests. The reaction of solketal with dimethyl carbonate (DMC)

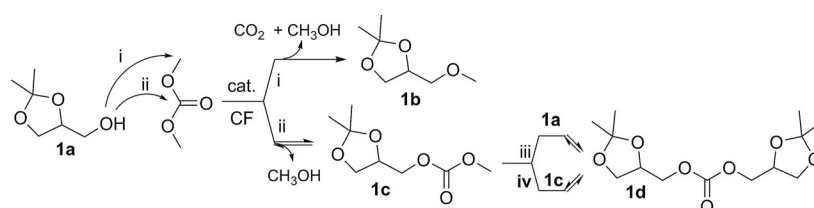
Table 1. Hydrotalcites used in this work.					
Entry	Sample label	MgO/Al ₂ O ₃ [%]	Surface area ^[a] [m ² g ⁻¹]	Source	Post-synthesis residues [%]
1	HT30	30:70 ^[b]	250	Pural® MG30, Sasol	
2	HT63	63:37 ^[b]	230	Pural® MG63, Sasol	Na: 1.5 × 10 ^{-3[a]}
3	HT70	70:30 ^[b]	180	Pural® MG70, Sasol	K: 1.7 × 10 ^{-3[a]}
4	KW2000	64:36 ^[b] (65:35) ^[c]	190	Kyowa Kagaku Kogyo Co. Ltd.	Na: 2.5 × 10 ^{-2[c]} K: 1.1 × 10 ^{-2[c]}

[a] Data specified by the supplier. [b] Ratio [wt%] specified by the supplier. [c] Determined by ICP-MS measurement.

was chosen as a model to investigate the activities of the different catalysts and the effects of four major reaction parameters, that is, temperature, pressure, time and reactant molar ratio.

CF tests over different catalysts

The performances of the FAU and HT catalysts in the above-described CF apparatus were compared. The temperature and pressure for the initial tests were selected according to our previous results obtained for the batch alkylation and CF transesterification reactions of glycerol acetals with dialkyl carbonates.^[10,16] In particular, the experiments were performed in the ranges $T=200\text{--}275\text{ }^{\circ}\text{C}$ and $p=5\text{--}50$ bar. Each of the investigated catalysts was used to fill the inner volume of the CF reactor as uniformly and completely as possible.^[17] Therefore, the amount of each solid sample was adjusted according to its apparent density: NaY, NaX, CsY, KW2000, HT30, HT63 and HT70 were used as such in slightly different quantities of 0.68, 0.54, 0.86, 0.52, 0.73, 0.51 and 0.85 g, respectively. Each catalyst was dehydrated under vacuum (70 °C, 18 mm, overnight) before use. In all of the tests, the same 1.83 M solution of solketal in DMC [DMC/solketal molar ratio (W) = 5] was fed to the reactor at a total volumetric flow rate (F) of 0.1 mL min⁻¹, which corresponds to a contact time of approximately 10 min. The excess DMC served both as a reagent and a carrier/solvent. During the CF experiments, samples of the mixtures were collected periodically at the reactor outlet for GC-MS analysis, which allowed for the evaluation of both the reaction conversion (measured with respect to solketal as the limiting reagent) and the product distribution. Each test was duplicated to check the reproducibility; in each reaction, a fresh sample from the same batch of catalyst was used.^[18]



Scheme 3. Major products of the CF catalytic reaction of solketal with DMC.

Several reactions occurred under the conditions explored; the double electrophilic reactivity of dimethyl carbonate accounted for the formation of *O*-methyl and transesterification derivatives, **1b** and **1c**, respectively (Scheme 3: paths i and ii). Subsequently, compound **1c** could plausibly undergo a further transesterification with solketal or a dismutation reaction to afford the symmetric carbonate product **1d** (Scheme 3: paths iii and iv). The structures of **1b**, **1c** and **1d** were assigned by GC-MS and NMR spectroscopy analyses and by comparison to previously synthesised authentic samples. Moreover, some unidentified side-products were also observed. These compounds are referred to as “others”, and their GC-MS data are consistent with a ring-opening reaction of the acetal ring followed by methylation and transesterification of the corresponding (linear) derivative.

At 250–275 °C and 10 bar, FAUs were unsuitable catalysts for the reaction investigated. At best, the conversion of solketal was moderate (60–70%). The more basic NaX and CsY systems were slightly more active than NaY but favoured the transesterification product **1c** with a selectivity of 60–70%.^[19] NaY improved the formation of the *O*-methyl derivative **1b** (up to 40%) but also induced side-reactions to afford a sizeable amount of unidentified byproducts. In all cases, the conversion and selectivity were steady after 180 min and did not vary substantially if the CF tests were prolonged to 18 h (Supporting Information, Figures S2a–b and Table S1).

This behaviour neatly contrasted with our previously reported results for the reaction of benzyl-type alcohols with DMC, through which the corresponding *O*-methyl ethers were achieved quantitatively and selectively in the presence of NaX and NaY catalysts.^[20] Unlike aromatic or benzyl substrates,^[14,21,22] solketal has a cycloaliphatic structure, which could be more weakly coordinated to the FAU surface and, thereby, alter the reaction outcome. On the basis of the hard and soft acids and bases (HSAB) principle, other authors have also proposed that hard nucleophiles such as aliphatic alcohols prefer the hard electrophilic site of DMC (i.e., the carboxyl carbon atom) rather than the softer methyl group.^[23]

The scenario changed completely in the presence of HTs. In particular, the use of KW2000 improved the conversion and, even more remarkably, the methylation selectivity. The reactions were performed under the same conditions as those for Figure 2b (275 °C, 10 bar, $W=5$, $F=0.1$ mL min⁻¹), but the reactions were performed for a longer time (18–20 h). The performances of the HT catalysts are summarised in Figure 1a and b with emphasis on KW2000.

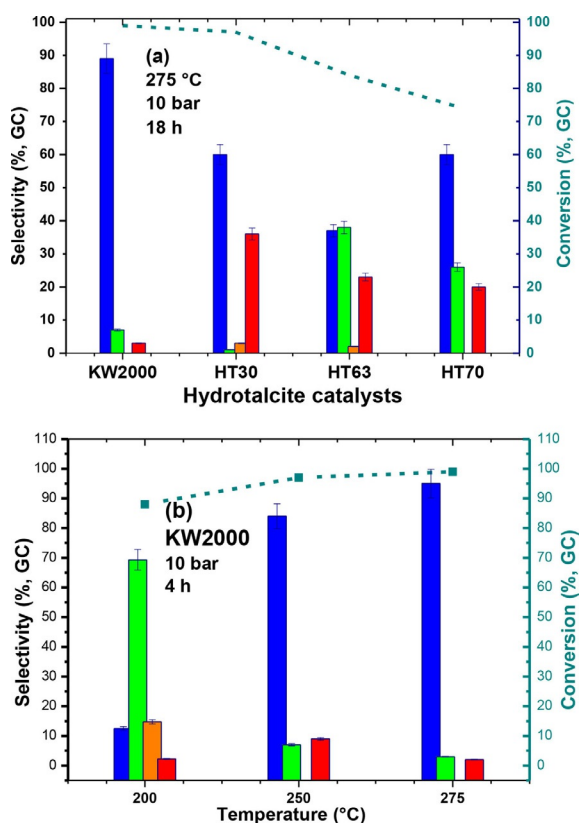


Figure 1. Trends for the conversion and product distribution for the CF reaction of solketal with DMC: (a) comparison of different HT catalysts at 275 °C and 10 bar; (b) effect of the temperature during catalysis by KW2000 at different temperatures. The coloured bars (from left to right) show the selectivity towards the *O*-methyl product (**1b**, ●), the transesterification or dismutation derivatives (**1c**, ● and **1d**, ●, respectively) and unidentified compounds (others, ●). The dashed line (from right to left) shows the trend of solketal conversion. DMC and solketal were used in a 5:1 molar ratio (W), and the total flow rate was 0.1 mL min⁻¹.

All hydrotalcites investigated were better catalysts than the FAUs, but KW2000 offered a performance far superior to those of the other HTs (HT30, HT63 and HT70; Figure 1a). The KW2000-catalysed reaction proceeded with a very good conversion and *O*-methylation selectivity of 99 and 89%, respectively (dashed green line and blue bar, Figure 1a). The ring of the reactant acetal was substantially preserved, and further transformations were avoided; only traces of the transesterification product **1c** were observed. The second best hydrotalcite, that is, HT30, still allowed an almost quantitative process (conversion 96%), although the methyl derivative **1b** did not exceed 60% of the total of the observed products (Figure 1a).

The reactions catalysed by KW2000 and HT30 were explored in greater depth through the analysis of samples of the mixture collected at the CF reactor every 60 min for 20 h (Figures S3a–b). In the presence of KW2000, a steady and almost complete conversion was obtained after just 1 h, whereas the *O*-methylation selectivity reached a maximum of 95% in 4 h and only decreased slightly to 87–89% at the end of the test (18–20 h; Figure S3a). For the HT-30-catalysed process, the conversion was below 80% in the first 4 h, and the transesterification compound, **1c**, was the dominant product (Figure S3b). After

18–20 h, the residual solketal was present in trace amounts (2–5%), and a steady formation of both **1b** and unidentified products was observed (≈ 60 and 40%, respectively). Although their product distributions were different, both reactions displayed an initial (induction) period during which mixtures of products formed. Thereafter, the conversion and selectivity stabilised, and the almost exclusive formation of ether **1b** was observed for KW2000. For this catalyst, three additional short experiments (4 h each) were performed to examine the effect of the temperature in the range 200–275 °C with the other conditions unaltered (10 bar, $W=5$, $F=0.1$ mL min⁻¹; Figure 1b). For KW2000 at 200 °C, the transesterification and disproportion reactions were the major transformations (green and ochre bars, Figure 1b). However, the *O*-methylation process was triggered by a temperature increase and was favoured progressively above 250 °C.

For KW2000, further tests were also devised to investigate the effects of the pressure and the DMC/solketal molar ratio W (see Figures S4a and b). At 275 °C ($W=5$, $F=0.1$ mL min⁻¹, 4 h), if the pressure was decreased or increased to 5 or 50 bar, the conversion diminished slightly (from 99 to $\approx 95\%$), but the methylation selectivity dropped from 95 to 75–80% because of the onset of transesterification and unidentified side-reactions. It is plausible that the pressure influenced the partition of the reactants between the liquid and the vapour phases and, consequently, the contact of solketal and DMC with the catalyst surface. We previously observed a similar behaviour during an investigation of the thermal (catalyst-free) transesterification of glycerol acetals and glycerol with DMC.^[24] However, at 275 °C and 10 bar ($F=0.1$ mL min⁻¹, 4 h), if W decreased from 5 to 1.1, both the conversion and the *O*-methylation selectivity decreased to 58 and 62%, respectively, and there was a significant formation of products **1c**, **1d** and “others”.

Two effects might plausibly account for this result at a constant F : (1) If more DMC is present ($W=5$), the rates (and conversion) of the DMC-mediated reactions are higher. Under these conditions, even though (reversible) transesterifications occurred, the corresponding products (**1c** and **1d**) were observed in only minor amounts, because these compounds were consumed by the onset of the parallel irreversible *O*-alkylation reaction, which proceeded almost to completion (Scheme 3 and Figures 1a, S3 and S4). However, for $W < 5$ and particularly at $W=1.1$, lower-energy-demanding reaction pathways, that is, transesterification processes, became more evident; therefore, the quantities of derivatives **1c** and **1d** increased. (2) A low DMC/solketal molar ratio ($W=1.1$ –2) not only disfavoured the solvation of the acetal by DMC and the mutual interactions between reactants but also facilitated the occurrence of intramolecular side-processes including, for example, the ring opening of solketal (“others” as byproducts) adsorbed over the catalyst surface.

CF tests with calcined HTs

If hydrotalcites are heated to approximately 200 °C, they release water; however, at approximately 300 °C (near the tem-

perature used in Figure 1) and above, a collapse of the typical layered structure of HTs occurs, and Mg/Al mixed oxides form.^[25] These facts prompted us to explore the catalytic activities of calcined hydrotalcites (c-HTs) in the reaction of solketal with DMC. The c-HTs were prepared by heating the Pural® (HT30, HT63 and HT70) and KW2000 solids at 450 °C in a dried air flow for 16 h.^[26] The c-HTs showed quite similar apparent densities, and the same amounts (0.5 g each) were used for the catalytic tests. In all cases, a 1.83 M solution of solketal in DMC ($W=5$) was fed to the reactor at $F=0.1 \text{ mL min}^{-1}$. The experiments proved that the calcined hydrotalcites, particularly c-HT30, improved the reaction outcome dramatically. The solketal conversion and the *O*-methylation selectivity increased, and the c-HT30 catalyst was also active at temperatures and pressures remarkably lower than those used previously. With the other conditions unaltered ($W=5$, $F=0.1 \text{ mL min}^{-1}$), the reactions could be run at temperatures and pressures as low as only 210 °C and 1 bar.

The performance of c-HT30 over 20 h on-stream is detailed in Figure 2, and the activities and *O*-methylation selectivities of

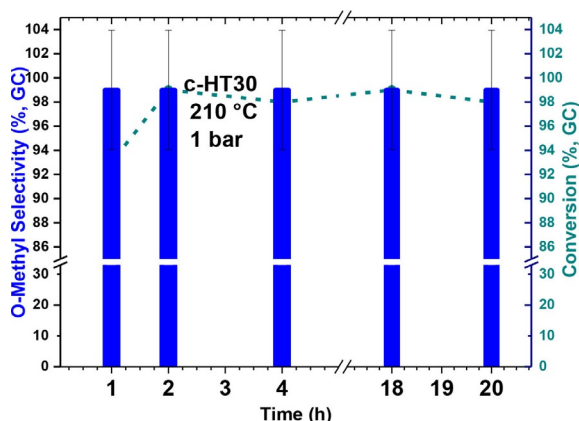


Figure 2. CF reaction of solketal with DMC in the presence of c-HT30 catalyst at 210 °C and ambient pressure. Trends of *O*-methylation selectivity and conversion of solketal with time (blue bars and dashed green profile). Other conditions: $W=5$, $F=0.1 \text{ mL min}^{-1}$.

different c-HTs are compared in Table 2. Each test was duplicated to check the reproducibility of the results.^[18] The outcome of the reaction catalysed by c-HT30 exemplifies one of the best reported *O*-methylation reactions of an alcohol-like func-

tion mediated by DMC. The solketal was transformed quantitatively to the methyl ether **1b**, and a steady efficiency was ensured for at least 20 h. The comparison of Figures 2, 1 and S2a and b also indicated that the catalytic properties of both HT30 and KW2000 were modified considerably not only by the calcination of the HTs but also by the thermal treatment during high-temperature (275 °C) reactions. At the same reaction temperature (210 °C) used for c-HT30, the other c-HT catalysts resulted in conversions and *O*-methylation selectivities not exceeding 88 and 27%, respectively, even at 10 bar (Table 2: compare c-HT70, c-KW2000 and c-HT63 in entries 2–4, columns 4–7). Minor improvements were achieved at 225 °C (entries 2–4, columns 8–11). The reaction proceeded with the complete conversion of solketal to the methyl derivative **1b** over all c-HTs catalysts only at 275 °C (10 bar, $W=5$, $F=0.01 \text{ mL min}^{-1}$).

The ability of calcined hydrotalcites to promote the investigated reaction was contrasted with other CF experiments in which the c-HTs were replaced by either MgO (0.85 g of a mixture of 60 wt% MgO with ground-glass Raschig rings) or a physical mixture of MgO and basic $\gamma\text{-Al}_2\text{O}_3$ in a 30:70 molar ratio (0.85 g), both of which mimicked the formal composition of HT30. Both of these solids were calcined at 450 °C for 6 h before use. Under the conditions described above (275 °C, 10 bar, $W=5$, $F=0.01 \text{ mL min}^{-1}$), the two catalysts gave modest results: the best one was MgO, for which the reaction proceeded with a conversion and *O*-methyl selectivity of only 80 and 48%, respectively. Although MgO and $\gamma\text{-Al}_2\text{O}_3$ were reported recently to catalyse both *O*- and *N*-alkylations mediated by DMC,^[27,28] these solids were clearly inadequate for the reaction investigated.

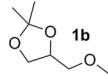
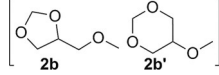
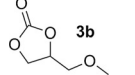
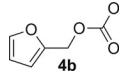
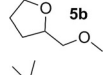
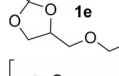
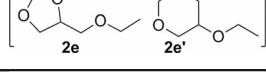
The study so far demonstrated that KW2000 and HT30 were the most promising catalysts. To continue our exploration of the potential of such materials, in particular the calcined system c-HT30, we focused the investigation on the scope and limitations of the CF-etherification of other OH-bearing bio-based derivatives with both dimethyl and diethyl carbonate.

Scope of the reaction: different reactants, mass balance and productivity

The substrates shown in Scheme 1, including glycerol formal (**2a+2a'**), glycerol carbonate (**3a**), and furfuryl and tetrahydrofurfuryl alcohols (**4a** and **5a**), were reacted with DMC or diethyl carbonate (DEC) under CF conditions. Accordingly, a homo-

Entry	Catalyst	p/t [bar h^{-1}]	Reaction temperature 210 °C			225 °C				
			Conversion ^[a] [%]	Selectivity ^[a] [%]		Conversion ^[a] [%]	Selectivity ^[a] [%]			
				1b	1c	others		1b	1c	others
1	c-HT30	10/18	99	99	–	–	99	99	–	–
2	c-HT70	10/18	88	27	49	24	95	40	42	18
3	c-KW2000	10/18	85	15	61	24	93	20	68	12
4	c-HT63	10/18	78	2	68	30	87	8	61	31

[a] Conversion of solketal and selectivity towards the *O*-methyl derivative **1b**, the transesterification compound **1c** and other products (including the disproportionation derivative **1d** and unidentified byproducts), respectively. Other conditions: $W=5$, $F=0.1 \text{ mL min}^{-1}$.

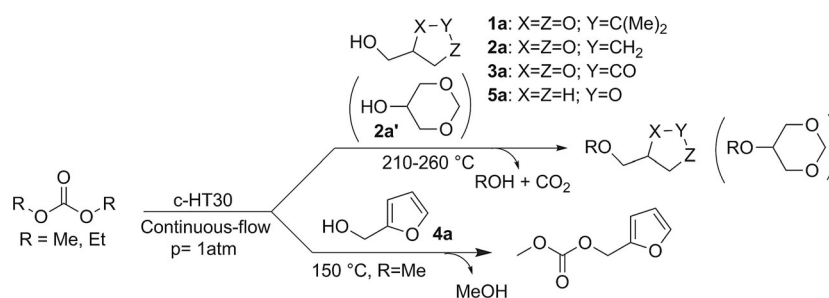
Table 3. The CF reactions of substrates 1a–5a with DMC and DEC in the presence of c-HT30 catalyst. ^[a]									
Entry	Substrate	Dialkyl carbonate	$W^{[b]}$	T [°C]	Conversion [%] ^[c]	Selectivity [%] ^[d]	Product Structure	$Y^{[e]}$ [%]	$P^{[f]}$ [g _{prod} g _{cat} ⁻¹ h ⁻¹]
1	1a	DMC	5	210	99	99		92	2.64
2	2a/2a'	DMC	5	220	99	99		81	1.92
3	3a	DMC	20	210	98	65		55	0.42
4	4a	DMC	10	150	88	91		80	1.26
5	5a	DMC	5	260	99	92		82	1.94
6	1a	DEC	5	250	99	99		92	2.04
7	2a/2a'	DEC	5	275	99	99		84	1.62

[a] Reactions were performed for 6 h (20 h for **1a**, entry 1) at ambient pressure and at $F=0.1$ mL min⁻¹. [b] Dialkyl carbonate/substrate molar ratio. [c] Conversion of the substrate (determined by GC). [d] Selectivity towards the shown product (determined by GC). [e] The isolated yield was evaluated by the workup of a mixture collected at the reactor outlet after 6 h (15 h for **1a**, entry 1). [f] The reaction productivities were calculated for isolated yields.

geneous solution of dialkyl carbonate and the substrate was delivered to the CF reactor filled with c-HT30 (0.5 g) as a catalyst for 6 h. The total flow rate was of 0.1 mL min⁻¹, and all of the CF tests were repeated twice to check their reproducibility. The reaction conditions, isolated yields (Y) and productivities (P : g products obtained in 1 h per g catalyst) for each of the studied processes are listed in Table 3, and the reactions and the structures of the products are summarised in Scheme 4. For completeness, the above-described results for the reaction of solketal with DMC are included in Table 3. The reactions could be performed at atmospheric pressure, but the operating temperature and the molar ratio of the reactants had to be optimised on a case-by-case basis in the ranges 210–275 °C and 5–20, respectively. Except for **4a**, quantitative conversions were reached for all of the substrates, and the O -alkylation selectivities were 65–99%. All of the products were isolated and

characterised by NMR spectroscopy and GC–MS (the details are provided in the Supporting Information).

Solketal and glycerol formal (**1a** and **2a/2a'**) could be converted quantitatively into the corresponding methyl and ethyl ethers (**1b** and **2b/2b'**) by using DMC and DEC as O -alkylating agents. From the results, two facts emerged: (1) Regardless of the dialkyl carbonate, the etherification of glycerol formal was more energy-demanding than that of solketal. Methyl and ethyl ethers **2b/2b'** and **2e/2e'** were obtained at 220 and 275 °C, respectively, whereas **1b** and **1e** formed at the lower temperatures of 210 and 250 °C (compare Table 3, entries 1 and 2 with 6 and 7). A similar difference was observed for the transesterification of glycerol acetals with DAICs.^[24] The higher density of glycerol formal (1.21 g mL⁻¹) with respect to that of solketal (1.07 g mL⁻¹) might play a role. (2) The syntheses of ethyl ethers required considerably higher temperatures (250–

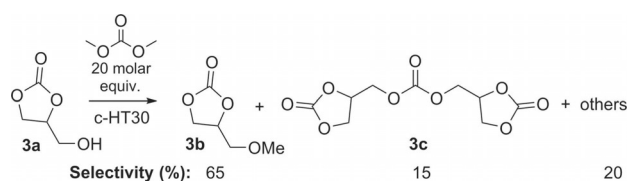


Scheme 4. The etherification of OH-bearing BBDs **1a–3a** and **5a** (top). The transesterification of furfuryl alcohol with DMC (bottom).

275 °C) than those for methyl ethers (210–220 °C; Table 3, compare entries 1 and 6 with 2 and 7). This result was in line with the trend noticed for several processes mediated by DAICs, including transesterifications, decarboxylations, etherifications and alkylations.^[10] Steric reasons probably account for the lower electrophilic reactivity of DEC compared with that of DMC. The products were recovered in good-to-excellent isolated yields (81–92%); however, the more volatile derivatives of glycerol formal gave slightly poorer results because of some technical difficulties with their separation from DMC or DEC (**2b/2b'**: 81%; **2e/2e'**: 84%; Table 3, entries 2 and 7).^[29] The isomeric ethers **2b/2b'** and **2e/2e'** were obtained in the same (3:2) relative ratio as that of the starting acetals **2a** and **2a'**.

The reaction productivity, calculated from the isolated yield, allowed further remarkable considerations: compared with the *P* values of 0.01–0.02 g_{prod}g_{cat}⁻¹h⁻¹ for the syntheses of compounds **1b** and **2b/2b'** by our previously reported batchwise (autoclave) method,^[16] the CF procedure boosted the productivity by a factor of 100–200 [to ≈ 2 g_{prod}g_{cat}⁻¹h⁻¹]; Table 3, entries 1 and 2] and, thereby, substantiated the synthetic potential of such a protocol. The overall mass balance for the alkylation of glycerol acetals was also validated by NMR spectroscopy of crude mixtures collected at the reactor outlet and gravimetric analyses of the catalytic bed before and after the CF tests; both of these checks indicated that neither heavy products nor noticeable coke formation (on the catalyst) occurred even after prolonged experiments (up to 20 h, Table 3, entry 1). A similar outcome was also observed for the CF reaction of tetrahydrofurfuryl alcohol (**5a**) with DMC, in which we obtained the corresponding *O*-methyl ether (**5b**) with 92 and 80% selectivity and isolated yield, respectively (Table 3, entry 5). However, a higher operating temperature of 250 °C was necessary.

The control of the chemoselectivity was significantly more difficult for the reactions of glycerol carbonate (**3a**) and furfuryl alcohol (**4a**). Glycerol carbonate was sensitive to competitive transesterification^[24b] and decarboxylation^[30,31] reactions to produce higher carbonate homologues and glycidol, respectively. In this case, 65% *O*-methylation selectivity was achieved at 210 °C in the presence of a large excess of the alkylating agent (Table 3, entry 3 and Scheme 5). Owing to dilution or solvation effects, these conditions contribute to minimise the contact between the glycerol carbonate and the catalytic surface and, thereby, limit undesired decarboxylation reactions. Of note, the methylation productivity (0.42) of the process was twice as much as the best value reported previously (0.21) for a batch reaction of glycerol carbonate with DMC catalysed by Al₂O₃.^[32]

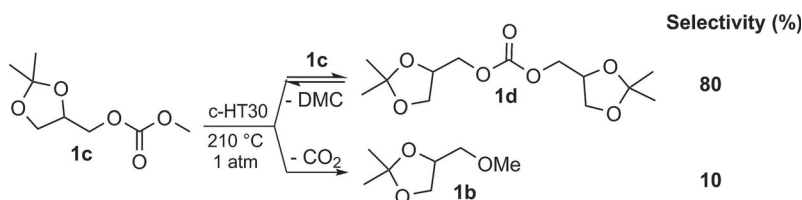


Scheme 5. The CF reaction of glycerol carbonate with DMC in the presence of c-HT30 (the structure of **3c** was assigned by GC-MS; the others were unidentified byproducts).

Furfuryl alcohol (**4a**) was too reactive to allow the formation of the corresponding alkyl ether. At $T \geq 180$ °C, the reaction of **4a** with DMC gave polymeric byproducts, which blocked the catalytic bed rapidly. However, at a lower temperature (150 °C), a highly selective transesterification provided (furan-2-yl)methyl methyl carbonate (**4b**) in 80% isolated yield (Table 3, entry 4). This equilibrium reaction was also favoured by a large excess of DMC (10 equiv. with respect to **4a**). Of note, all of the previously reported syntheses of **4b** were based on the reaction of furfuryl alcohol with a harmful phosgene derivative such as methyl chloroformate;^[33] the process described here is the first successful example of the same preparation with DMC as a non-toxic reagent.

The results listed in Table 3 proved that c-HT30 was an efficient catalyst and that it could be recycled without loss of performance. For example, once the CF alkylation of solketal was run for 20 h (entry 1), a simple cleaning cycle of the catalytic bed with methanol (50 mL at 1 mL min⁻¹, 50 °C, atmospheric pressure) restored the system to its initial conditions, and the same reactions or a new reaction (e.g., the alkylation of glycerol formal) could be performed. No activity differences were observed if a used c-HT30 catalyst was compared to a freshly calcined HT30 sample; therefore, the CF procedure is robust. This was further substantiated by the very low metal leaching from the catalyst: after the test of entry 1 (Table 3), ICP-MS measurements demonstrated that the Al and Mg concentrations in the stream recovered at the outlet of the reactor were 40 and 85 ppb, respectively (see Experimental Section and Supporting Information for details). The estimated mass loss of the catalytic bed corresponded to 38 μg per 20 working hours. Very low levels of metal leaching were observed previously for others reactions catalysed by HT-derived Mg/Al mixed oxides: two examples are the transesterifications of natural fats and liquid-phase Michael additions.^[34] After the vacuum distillation of the mixtures collected at the reactor outlet, it was also estimated that up to 80% of the unreacted DMC (and its azeotrope with MeOH)^[35] and DEC could be recovered and recycled with minimal waste generation.

Overall, the CF procedure was versatile and suitable for both carbonates and alcohols. In particular, c-HT30 provided a rational long-term stability and selectivity (with no appreciable leaching or poisoning) as well as a productivity that could be orders of magnitude higher than that achieved by batch alkylation methods. To the best of our knowledge, a result comparable to that of c-HT30 was reported only for the continuous-flow *O*-methylation of primary alcohols with DMC catalysed by γ-Al₂O₃.^[28] However, this protocol could hardly be extended: *sec* alcohols gave substantial side-reactions through eliminations to afford alkenes promoted by the acidity of the catalyst;^[36] moreover, even at 150 °C, DMC underwent an extensive decarboxylation reaction to afford dimethyl ether.^[37] For the functionalised alcohols used in this study, γ-Al₂O₃ would have posed a chemoselectivity concern; glycerol acetals (solketal and glycerol formal) and furfuryl alcohol are extremely sensitive to ring aperture and polymerisation reactions catalysed by acids, whereas glycerol carbonate would release CO₂ rapidly.



Scheme 6. The CF reaction of **1c** over c-HT30 at 210 °C and ambient pressure. Cyclohexane was used as a solvent (5 equiv. with respect to **1c**). Total flow rate: 0.1 mLmin⁻¹.

It should be noted that the decarboxylation of dialkyl carbonates may be catalysed by FAUs^[10] or by hydrotalcites as such.^[38] However, under the CF conditions explored here, we observed that calcined HTs were far less efficient for the same process. This was corroborated by an additional test in which solketal methyl carbonate (**1c**) was reacted at 210 °C and ambient pressure over a catalytic bed of c-HT30. At a conversion of 75%, **1c** underwent a predominant disproportionation reaction towards bis[(2,2-dimethyl-1,3-dioxolan-4-yl)methyl] carbonate (**1d**, 80%) rather than the decarboxylation to derivative **1b** (10%, Scheme 6). Product **1d** was isolated in a 58% yield and characterised by GC-MS and NMR spectroscopy (see Supporting Information). Albeit indirectly, this test confirmed that c-HT30 could also improve the efficiency of the alkylation reactions desired here.

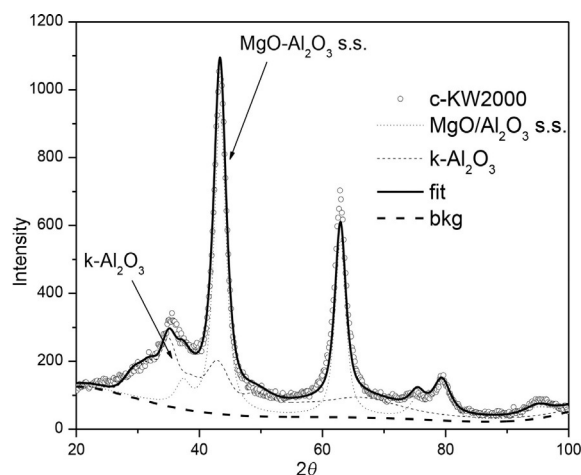


Figure 4. XRD pattern and Rietveld fit of c-KW2000 ($R_{wp} = 9.5\%$).

Characterisation and role of the catalyst

The performance of the investigated catalysts was consistent with structural modifications induced by calcination and, potentially, during the reaction itself. Therefore, the two most active systems, KW2000 and HT30, were subjected to a more in-depth analysis and characterisation. A total of four samples were examined for XRD analyses. Two of them (f-KW2000 and f-HT30) were fresh solids that had never been used for catalytic tests, and the other two specimens (c-KW2000 and c-HT30) were calcined catalysts used for reactions under the conditions for Table 2 (for details, see Table S2). The XRD patterns for the fresh materials are shown in Figure 3, and those of the calcined solids are shown in Figures 4 and 5.

The fresh solids contained at least two phases. The hydrotalcite structure (ICSD 81963) was present along with large fractions of periclase [MgO, ICSD 9863; (60 ± 1) wt%] in f-KW2000

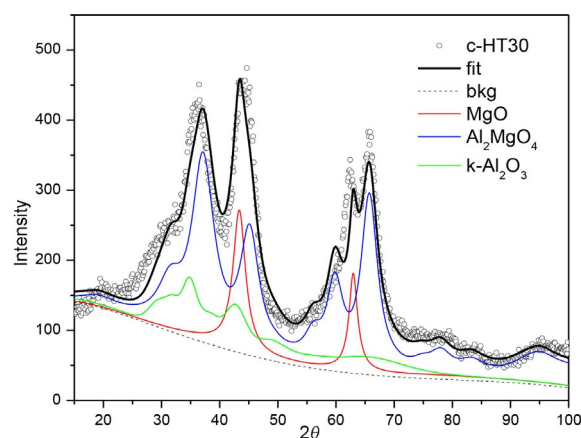


Figure 5. XRD pattern and Rietveld fit of c-HT30 ($R_{wp} = 11.6\%$).

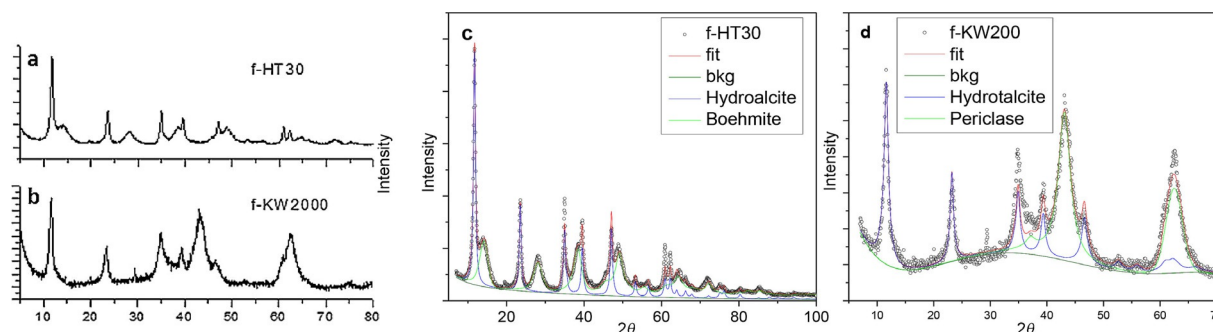


Figure 3. XRD patterns (left) and Rietveld fits (right) for f-HT30 and f-KW2000 samples.

and boehmite [aluminum oxide hydroxide, ICSD 36340; (53 ± 1) wt%] in f-HT30. The quantitative relationships between the constituent phases were obtained by the Rietveld analysis shown in Figure 3 c and d. For comparison, XRD patterns were also acquired for fresh solid samples of HT63 and HT70, and these materials were single-phase hydrotalcites (for further details, see Figure S31).

The XRD pattern of c-KW2000 showed the presence of cubic MgO (periclase) along with an extremely dispersed or amorphous phase responsible for a broad peak at $2\theta = 35^\circ$ (Figure 4). The XRD pattern was typical of c-HT systems characterised by an Al/(Al+Mg) molar fraction of up to approximately 50% (≈ 55 wt% of Al_2O_3).^[39,40] A Rietveld analysis was then performed with the following considerations: (1) In addition to MgO, both Al_2O_3 and the spinel Al_2MgO_4 would be the other most probable components of the c-KW2000 system.^[41] (2) If the thermal degradation of a hydrotalcite occurred at 300–500 °C, metastable phases of MgO and finely dispersed Al_2O_3 or solid solutions of $\text{Al}_2\text{MgO}_4/\text{Al}_2\text{O}_3$, $\text{MgO}/\text{Al}_2\text{O}_3$ or both could form.^[42] Among the aluminas, k- Al_2O_3 (ICSD 94485) gave the best fit of the XRD pattern (Figure 4). It was also noticed that the refined cell for MgO was smaller [(4.190 ± 0.001) Å] than that of pure MgO (4.2112 Å) and, thereby, indicated the formation of a solid solution (ss) of alumina in magnesia in which the Al atoms occupied 15% of the cationic sites.^[42] By assuming that the ss dissolved the Al_2O_3 phase, the quantitative Rietveld analysis of Figure 4 allowed us to estimate proportions of Al_2O_3 (39 wt%) and MgO (61 wt%) that were very close to the nominal composition of the sample. This indirectly supported the presence of almost pure Al_2O_3 as the amorphous phase. Finally, the ss was totally absent in the fresh sample of KW2000 (Figure 3 b), in which periclase showed a unit-cell parameter of (4.213 ± 0.002) Å. The XRD patterns of the c-HT63 and c-HT70 solids were very similar to that of c-KW2000 (see Figure S32).

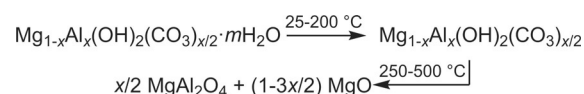
By contrast, the diffraction pattern of c-HT30, which contains a higher fraction of Al, was totally different (Figure 5). Rietveld analyses were performed as mentioned above and allowed us to identify the presence of a $\text{MgO}/\text{Al}_2\text{O}_3$ ss, the spinel Al_2MgO_4 and k- Al_2O_3 , and the corresponding amounts of these three phases were estimated to be 15, 63 and 22 wt%, respectively. Although the obtained fit was not as good as the previous one (cf. the R_{wp} indices of Figures 4 and 5), the calculated proportions of Al_2O_3 (69 wt%) and MgO (31 wt%) were very close to those of the nominal composition of the sample.

The BET results were in substantial agreement with the surface-area trend that is usually observed for fresh and calcined HTs.^[25a,43] Although the fresh samples of KW2000 and HT30 were not pure hydrotalcite phases, an increase of S_{BET} was noticed once both solids were calcined at 450 °C (Table S2: 108 and 199 m^2g^{-1} for f- and c-KW2000 and 136 and 247 m^2g^{-1} for f- and c-HT30, respectively).

Overall, the comparative bulk characterisation indicated that fresh f-KW2000 and f-HT30 acted as precursors of active catalysts for the O-alkylation reactions investigated here. Such active phases were composed of solid solutions of Mg/Al oxides along with amorphous alumina and formed during the thermal treatment of the hydrotalcites investigated.^[27,39,40] This

matched the behaviour described previously, as is summarised in Scheme 7.^[25]

Above 250 °C, HTs decompose because of the release of water and extensive dehydroxylation and decarbonation reac-



Scheme 7. The decomposition of Mg–Al hydrotalcite.

tions of the intralayer OH^- and CO_3^{2-} anions. However, as the produced phases (MgAl_2O_4 , Al_2O_3 or Al-doped MgO) often have small nuclei, they are hardly distinguishable from each other;^[44,45] therefore, the outcome of the thermal process and the precise nature of the mixed oxides is still not resolved completely. These considerations allowed us to formulate a hypothesis to explain why KW2000 could be used as such in the investigated O-alkylation reactions (Figure 1: f-KW2000), whereas HT30 was active only upon calcination (Figure 2 and Table 3). As the two solids showed quite different chemical compositions in which the layered HT structure coexisted with large proportions of periclase in f-KW2000 or boehmite in f-HT30 (Figure 3 a and b, respectively), it was plausible that the breakdown shown in Scheme 7 occurred under different conditions. For f-KW2000, the process could be completed during the CF alkylation reactions at 275 °C, whereas the collapse of f-HT30 required a more energy-demanding transformation, which was achieved only during a high-temperature calcination at 450 °C.

Another question was the different performances of the investigated c-HT systems. Mixed Mg/Al oxides obtained through the calcination of HTs are often defined as amphoteric solids.^[27,40,46] This dual (acid/base) activity has been invoked to account for the nucleophilic and electrophilic activation of organic substrates promoted by c-HTs in several model reactions including transfer hydrogenations and aldol condensations of ketones,^[27,47] transesterification and carbonylation processes^[48] as well as eliminations and condensations of alcohols.^[43,49]

The basicity of c-HT systems has been the subject of many fundamental investigations, and it is generally agreed that basic sites of different strength can be defined including OH groups (weak), Mg–O or Al–O pairs (medium) and low-coordinate O^{2-} anions (strong).^[25,39,50] In this respect, the densities of total basic sites determined from the CO_2 temperature-programmed desorption (TPD) profiles of HT30 and HT70 solids after calcination at 450 °C were 1.35 and 3.00 $\mu\text{mol m}^{-2}$, respectively.^[51] This finding was consistent with the Mg/Al ratios of the samples: the higher the Al content (the more electronegative metal cation), the higher the nucleation of Al-rich phases and the lower the average basicity of the solid.^[27,40,47] In particular, the segregation of a large amount of a spinel phase observed through the XRD analysis of c-HT30 (Al_2MgO_4 : 63 wt%; Figure 5) probably indicated a partial coverage of the sites at the surface of MgO; therefore, the basicity would be lower than that of c-HT70 solid (the latter was composed mostly of a solid solution of alumina in magnesia: Figure S32). An exten-

sive analysis of these aspects was performed by Cavani et al.,^[25,50,52] who concluded that the Al/Mg ratio of the c-HTs induced a variability to the surface properties. However, in the range $2.0 < \text{Mg}/\text{Al} < 3.5$, all materials possessed basic sites mostly of medium strength, whereas Lewis-acid sites were manifest at low Mg/Al ratios in the form of coordinatively unsaturated Al^{3+} species. Moreover, the c-HTs were less basic than MgO. The same authors then proposed that a cooperative mechanism through a synergetic effect of the basic and Lewis-acidic sites could explain the selective *O*-methylation of phenol with methanol in the gas phase in the presence of c-HTs of Mg/Al = 2 as catalysts.^[52]

A similar formulation appeared consistent with the behaviour of the c-HTs shown in Figure 2 and Tables 2 and 3. Clearly, the results could not be attributed to a purely basic mechanism, as the best-performing catalyst c-HT30 was less basic than c-HT70 and far less basic than pure MgO. On the other hand, among the tested c-HTs, c-HT30 had not only a different bulk structure (Figure 5) but also a lower Mg/Al ratio, which could plausibly favour the occurrence of Lewis-acid sites. c-HT30 apparently displayed the best compromise of acid-base properties for the hypothesised mechanism shown in Scheme 8.

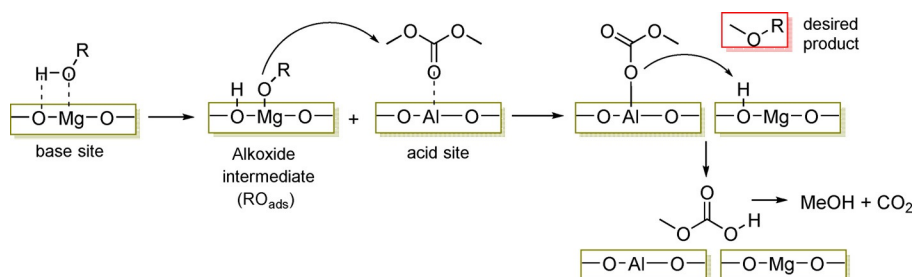
Both nucleophilic and electrophilic partners were activated by the catalyst. After the adsorption of an OH-bearing BBD (ROH: Scheme 1) at a Brønsted-basic site (e.g., Mg–O pairs), a deprotonation reaction followed to form the alkoxide intermediate RO_{ads} . The dialkyl carbonate (DMC in Scheme 8) was activated by the Lewis-acid sites (Al^{3+} cations) in the HT framework. Previously, we observed an electrophilic activation of DAICs by metal cations for FAU catalysts.^[22] Then, RO_{ads} undergoes a $\text{B}_{\text{AC}}2$ -type reaction with the adsorbed DMC to produce the desired methyl ether (ROME) and methyl hydrogen carbonate (MeOCO_2H). The latter is an unstable derivative and decomposes spontaneously into MeOH and CO_2 . RO_{ads} could also attack the carboxyl carbon atom of DMC to form the corresponding transesterification product (ROCO_2Me ; $\text{B}_{\text{AC}}2$ mechanism, see Scheme 3). However, the equilibrium of the transesterification process is shifted by the irreversible *O*-methylation reaction. The product distribution is also directed by the temperature. In line with previously reported results,^[3,16,10,14,33] alkylation and transesterification processes involving DAICs are discriminated between on the basis of their different energy demands, and methylations occur only at relatively high temperatures, usually above 150 °C.

A different situation was manifest for the four fresh HT solids investigated here, of which f-KW2000 was the best catalytic system (Figure 1). As mentioned above, the composition of f-KW2000 with a large excess of periclase (Figure 3b) could facilitate the decomposition of the solid towards a catalytically active phase ($\text{MgO}/\text{Al}_2\text{O}_3$ ss) even at the temperature of 275 °C used for the CF tests. However, KW2000 showed remarkable similarities to the HT63 and HT70 samples with comparable Mg/Al ratios (Table 1) and the bulk structure obtained by calcination (see Figures 4 and S32). This was further substantiated by the similar catalytic performances of the three calcined solids (c-KW2000, c-HT63 and c-HT70) in the *O*-methylation of solketal (Table 2). Therefore, although f-KW2000 could be converted into a catalyst at 275 °C (and 10 bar), the corresponding Mg/Al oxide active phase had to be more basic; consequently it was less efficient than c-HT30.

The effect of post-synthetic alkaline impurities on the catalytic activities of c-HTs was finally considered. Although doping with alkali-metal carbonates and hydroxides increases the basicity and the activity of HT systems, the necessary quantity of alkaline dopants must corresponded to an alkali-metal (Na, K) content of 0.5–10 wt%,^[53] These values were at least 250- and 20-fold higher than those of HT30 and KW2000, respectively (Table 1). Reasonably, the alkalinity from the residual Na or K salts in the investigated catalysts had a negligible role in the catalysis of the *O*-alkylation reactions with DAICs.

Conclusions

The investigation integrates an archetypical green reaction involving non-toxic and renewable reactants with an efficient continuous-flow (CF) procedure for the synthesis of alkyl ethers of a class of biobased derivatives. Calcined hydrotalcites (HTs), particularly c-HT30, are effective for highly chemoselective transformations: functionalised biobased alcohols and dialkyl carbonates are activated towards *O*-alkylations with respect to the competitive transesterifications and other side-reactions including the ring opening of acetal functions, decarboxylations of dialkyl carbonates and oligo- or polymerisations. An *O*-alkylation selectivity as high as 99% at complete conversion was achieved. To the best of our knowledge, this result has no precedent in the class of biomass-derived compounds investigated. The analyses of the bulk structures of the fresh and calcined hydrotalcites investigated here are consistent with the formation of catalytically active phases constituted by



Scheme 8. Proposed mechanism for the reaction of OH-bearing BBDs (ROH) and DMC at the HT surface.

mixed Al/Mg oxides. These originate either upon calcination or simply through heating to the reaction temperature, and their composition varies between the different HTs. The activity of the best catalyst (c-HT30) is consistent with both a lower density of basic sites and a more pronounced acid character than those of the other solids of the family. Overall, the CF protocol provides multiple advantages, of which the most relevant ones include the high process safety, the recyclability of the solvents and unconverted reagents, the reuse of the catalysts and the simplification of downstream operations for the isolation and purification of products to improve the productivity (greater by orders of magnitude) with respect to those of batch methods.

Experimental Section

General

Solketal (**1 a**), glycerol formal (GlyF, **2 a+2 a'**), tetrahydrofurfuryl alcohol (**4 a**), furfuryl alcohol (**5 a**), dimethyl carbonate (DMC), diethyl carbonate (DEC) and MgO were ACS-grade from Aldrich. If not otherwise specified, they were employed without further purification. Glycerol carbonate (**3 a**) was from JEFFSOL[®] and used as received. Solketal methyl carbonate (**1 c**) was prepared through the transesterification reaction of Solketal with DMC by a modification of a method developed by us.^[16]

GC–MS (EI, 70 eV) analyses were performed with an HP5-MS capillary column ($L=30$ m, $\varnothing=0.32$ mm, film=0.25 μm), and GC analyses with a flame ionisation detector (CG/FID) were performed with an Elite-624 capillary column ($L=30$ m, $\varnothing=0.32$ mm, film=1.8 μm). The ¹H NMR spectra were recorded at 400 or 300 MHz, and the ¹³C NMR spectra were recorded at 100 MHz; the chemical shifts are reported downfield from tetramethylsilane (TMS), and CDCl₃ was used as the solvent.

Catalysts

Faujasites of formula $M_z[(\text{AlO}_2)_z(\text{SiO}_2)_w]_n \cdot m\text{H}_2\text{O}$ ($M=\text{Na, Cs}$; X- and Y-type: $z=86$ and 56 , $w=104$ and 136 , $m=264$ and 250 , respectively) included NaX and NaY faujasites from Aldrich and a CsY zeolite synthesised by a conventional ion-exchange reaction of NaY with aq CsCl.^[18] The percentage of ion exchange ($\text{Na}^+ \rightarrow \text{Cs}^+$) was 58%, as evaluated through atomic emission according to a procedure that we reported previously.^[54] Before use, they were dehydrated under vacuum (70 °C, 18 mm, overnight).

According to the specifications provided by the manufacturers, the HTs were aluminium magnesium hydroxy carbonate hydrates of formula $\text{Mg}_{2x}\text{Al}_2(\text{OH})_{4x+4}(\text{CO}_3)_n \cdot n\text{H}_2\text{O}$ ($x=0.5\text{--}2.3$). Four commercial HTs were considered (their Mg/Al molar ratios are given in parentheses), namely, KW2000 (1.8), PURAL[®] MG 30 (0.5), MG 63 (1.9) and MG 70 (2.3). KW2000 was from Kyowa Chemical Industry Co., Ltd., whereas the PURAL[®] MG solids were from CONDEA/Sasol Germany GmbH, Inorganic Specialty Chemicals. The carbonate contents were approximately 10 wt%, and the maximum losses on ignition (3 h, 1000 °C) were in the 40–45% range. All HTs were used both as received and after calcination. If used as received, the solids were dehydrated under vacuum (70 °C, 18 mm, overnight) before they were loaded into the CF reactor. Otherwise, the calcination treatment was performed according to a procedure for HTs that we reported previously:^[21] solid samples (5 g) were heated in a quartz reactor (in the upright position) under a flow of dry air at 450 °C for 16 h. The heating rate was 30 °C min⁻¹.

Catalyst characterisation

Nitrogen adsorption–desorption isotherms were obtained at the liquid nitrogen temperature with a Micromeritics ASAP 2010 system. Each sample was degassed at 130 °C overnight before the measurement of the N₂ physisorption isotherm. From the data, the BET equation was used to calculate the specific surface areas.

The X-ray powder diffraction (XRPD) patterns were recorded with a Philips X'Pert powder diffractometer (Bragg–Brentano parafocusing geometry). Nickel-filtered CuK α 1 radiation ($\lambda=0.15406$ nm) and a voltage of 40 kV were employed. The XRD patterns were collected for all fresh (as-received) hydrotaalcites and the corresponding calcined solids.

The ICP-MS analyses were performed with a PerkinElmer Nexion 300XX instrument.

CF Apparatus

The apparatus used for the investigation was assembled in-house, as shown in Figure S1. An HPLC pump was used to deliver the liquid reactants to a stainless-steel tubular reactor ($L=12$ cm, $\varnothing=1/4"$, 1.16 cm³ inner volume) containing the catalyst, the amount of which was chosen on the basis of the apparent densities of the hydrotaalcites and faujasites. Typical catalyst loadings were in the range 0.5–0.85 g (see Figures 1 and 2 and Tables 2 and 3). The reactor was placed in the upright position in a thermostatted oven and heated to the desired temperature. A Swagelok back-pressure regulator (BPR) at the outlet of the reactor was used to keep the pressure constant over the whole system throughout the reaction. For experiments at ambient pressure, the BPR was bypassed. A Rheodyne Model 7725i injector equipped with a 10 μL sample loop was placed before the BPR and used for sampling.

SAFETY WARNING: Operators of high pressure equipment should take proper precautions to minimise the risk of personal injury.^[55] The individual components that we describe work well, but they are not necessarily the only equipment of this type available.

General procedure for the CF reactions of **1 a**, **2 a+2 a'**, **3 a**, **4 a**, **5 a** with DMC

A typical reaction with the CF apparatus described above was performed through the following procedure. The oven was set at a temperature of 150 °C, and N₂ was flushed through the system for 1 h. Then, the reaction mixture (dialkyl carbonate and the bio-based alcohol) was flowed for 10 min at 1 mL min⁻¹, and the BPR and oven were set to the operating pressure and temperature (5–60 bar and 150–300 °C, respectively). Once T and p were stable, the reactant flow was adjusted to the desired rate (0.07–0.2 mL min⁻¹). The reaction mixture was collected through a Rheodyne[®] valve (7725i fitted with a 10 μL sample loop) at time intervals of approximately 30 min, diluted with diethyl ether (1.5 mL) and analysed by GC/FID or GC–MS.

Change of reaction conditions: The oven and the BPR were set to the new desired T and p values, respectively. Under these conditions, the reactant mixture was flushed for 10 min at 1 mL min⁻¹. Then, the flow was adjusted to the chosen rate, and a new experiment was started.

System cleaning and restart: At the end of each experiment, the oven and the BPR were set to 50 °C and atmospheric pressure, respectively, and a cleaning solution of methanol (50 mL at 1 mL min⁻¹) was flowed through the system. The pump was then stopped, and the oven was allowed to cool to RT. The CF reactor

was then disassembled, and the catalytic bed could be replaced by a fresh one.

Reaction of Solketal (1a) and DMC with alkali-metal-exchanged faujasites as catalysts

The above-described procedure was used to test Faujasites as catalysts. Before use, each zeolite was dehydrated under vacuum (70 °C, 18 mm, overnight): NaY, NaX and CsY (0.68, 0.54 and 0.86 g, respectively) were charged in the CF reactor. In all tests, a 1.83 M solution of solketal in DMC [DMC/solketal molar ratio (W)=5] was fed to the reactor at $F = 0.1 \text{ mL min}^{-1}$. The CF reactions were performed under a constant pressure of 10 bar, and T was set to 250 or 275 °C. The experiments were followed for 3 h. Two additional runs with the NaY and NaX catalysts were performed for 18 h.

Reaction of Solketal (1a) and DMC with hydrotalcites

As-received hydrotalcites: The HTs were dehydrated under vacuum (70 °C, 18 mm, overnight): KW2000, HT30, HT63 and HT70 (0.52, 0.73, 0.51 and 0.85 g, respectively) were used for the CF tests. A 1.83 M solution of solketal in DMC ($W=5$) was fed to the reactor at $F=0.1 \text{ mL min}^{-1}$. At 275 °C, reactions were performed under a constant pressure of 10 bar and followed for 18 h (Figure 3a). For KW2000, additional experiments were performed under the following conditions: 1) $T=200$ and 250 °C, $p=10$ bar, $W=5$, $F=0.1 \text{ mL min}^{-1}$; 2) $T=275$ °C, $p=5$ and 50 bar, $W=5$, $F=0.1 \text{ mL min}^{-1}$; 3) $T=275$ °C, $p=10$ bar, $W=1.1, 2, 3.5$, $F=0.1 \text{ mL min}^{-1}$.

Calcined hydrotalcites: After calcination at 450 °C (see above for details), each solid (c-KW2000, c-HT30, c-HT63, and c-HT70; 0.5 g) was used for the CF tests. In all cases, a 1.83 M solution of solketal in DMC ($W=5$) was fed to the reactor at F of 0.1 mL min^{-1} . At 10 bar, the reactions catalysed by c-KW2000, c-HT30, c-HT63 and c-HT70 were run at 210, 225, and 275 °C for 18 h. For c-HT30, experiments were also performed at 210 °C and atmospheric pressure.

Two additional reactions were also conducted in which the c-HT catalysts were replaced by MgO (0.85 g) or a physical mixture of MgO and basic $\gamma\text{-Al}_2\text{O}_3$ (particle size: 50–200 μm , surface area: $130 \text{ m}^2 \text{ g}^{-1}$, pH 9.5 ± 0.3) in a 30:70 molar ratio (0.85 g). Both MgO and the MgO/ $\gamma\text{-Al}_2\text{O}_3$ mixture were calcined at 450 °C for 6 h before use. Then, the CF tests were run at 275 °C, 10 bar, $W=5$, and $F=0.01 \text{ mL min}^{-1}$.

Different substrates and carbonates

Reaction of Solketal and diethyl carbonate

According to the above-described general procedure, the reactions of glycerol acetals (1a and 2a+2a') were performed with DEC and c-HT30 (0.5 g) as the alkylating agent and catalyst, respectively. The CF reactions were performed at 250 and 275 °C and ambient pressure. A mixture of DEC and the chosen glycerol acetal in a 5:1 molar ratio was delivered at 0.1 mL min^{-1} to the CF reactor.

Different substrates

According to the above-described general procedure, the reactions of DMC with glycerol formal (2a+2a'), glycerol carbonate (3a), furfuryl alcohol (4a) and tetrahydrofurfuryl alcohol (5a) were investigated in the presence of c-HT30 (0.5 g) as a catalyst. The reactions

were optimised case-by-case under the following conditions: 1) 220 °C, 1 bar, glycerol formal/DMC in a 1:5 molar ratio; 2) 210 °C, 1 bar, glycerol carbonate/DMC in a 1:20 molar ratio; 3) 150 °C, 1 bar, furfuryl alcohol/DMC in a 1:10 molar ratio; 4) 260 °C, 1 bar, tetrahydrofurfuryl alcohol/DMC in a 1:5 molar ratio. The flow rate was set to 0.1 mL min^{-1} in all cases.

The isolation and characterisation of all of the products (1b, 2b+2b', 3b, 4b, 5b, 1e, and 2e+2e') by NMR spectroscopy and GC-MS is reported in the Supporting Information.

Acknowledgements

MIUR (Italian Ministry of University and Research) is acknowledged for funding the PhD program of L.C. through "Borse agiuntive di dottorato, fondo giovani". Dr. Roberto Clerici from Sasol Italy SpA is gratefully acknowledged for his generous supply of Pural® hydrotalcites and the discussion of the properties of these solids. Dr. Alexander Malyschew from Sasol Germany GmbH is also acknowledged. Finally, Mr. Tom Savage (University of Sydney) is acknowledged for his support with the ICP analyses.

Keywords: alkylation • aluminium • biomass • continuous flow • hydrotalcites

- [1] a) T. Werpy, G. Petersen, A. Aden, J. Bozell, J. Holladay, J. White, A. Mannheim, D. Eliot, L. Lasure, S. Jones in *Top Value Added Chemicals from Biomass: Volume 1—Results of Screening for Potential Candidates from Sugars and Synthesis Gas*, US DOE (DOE/GO-102004-1992), Washington, DC, **2004**; b) J. Bozell, G. R. Petersen, *Green Chem.* **2010**, *12*, 539–554.
- [2] T. J. Farmer, M. Mascal in *Introduction to Chemicals from Biomass*, 2nd ed. (Eds.: J. Clark, F. Deswarte), Wiley, Chichester, **2015**.
- [3] P. Tundo, M. Selva, *Acc. Chem. Res.* **2002**, *35*, 706–716.
- [4] a) L. Moity, A. Benazzou, V. Molinier, V. Nardello-Rataj, M. K. Elmekdem, P. de Caro, S. Thiébaud-Roux, V. Gerbaud, P. Marion, J.-M. Aubry, *Green Chem.* **2015**, *17*, 1779–1792; b) W. K. Teng, G. C. Ngoh, R. Yusoff, M. K. Aroua, *Energy Convers. Manage.* **2014**, *88*, 484–497; c) M. O. Sonnati, S. Amigoni, E. P. Taffin de Givenchy, T. Darmanin, O. Choulet, F. Guittard, *Green Chem.* **2013**, *15*, 283–306; d) *Advances in Biorefineries: Biomass and Waste Supply Chain Exploitation* (Ed.: K. W. Waldron), Woodhead Publishing, Cambridge, **2014**.
- [5] M. Pagliaro, M. Rossi, *The Future of Glycerol*, 2nd ed., RSC Publishing, Cambridge, **2010**.
- [6] a) M. Balakrishnan, E. R. Sacia, A. T. Bell, *Green Chem.* **2012**, *14*, 1626–1634; b) Y. Gu, F. Jerome, *Chem. Soc. Rev.* **2013**, *42*, 9550–9570; c) R. Mariscal, P. Maireles-Torres, M. Ojeda, I. Sádaba, M. López Granados, *Energy Environ. Sci.* **2016**, *9*, 1144–1189.
- [7] a) W. G. Trindade, W. Hoareau, J. D. Megiatto, I. A. T. Razera, A. Castellan, E. Frollini, *Biomacromolecules* **2005**, *6*, 2485–2496; b) W. Chaikittisilp, K. Ariga, Y. Yamauchi, *J. Mater. Chem. A* **2013**, *1*, 14–19; c) L. Pranger, R. Tannenbaum, *Macromolecules* **2008**, *41*, 8682–8687.
- [8] M. Chatterjee, H. Kawanami, T. Ishizaka, M. Sato, T. Suzuki, A. Suzuki, *Catal. Sci. Technol.* **2011**, *1*, 1466–1471.
- [9] a) M. Sutter, E. D. Silva, N. Duguet, Y. Raoul, E. Metay, M. Lemaire, *Chem. Rev.* **2015**, *115*, 8609–8651; b) A. E. Díaz-Álvarez, J. Francos, B. Lastra-Barreira, P. Crochet, V. Cadierno, *Chem. Commun.* **2011**, *47*, 6208–6227; c) B. J. Nikolau, M. A. Perera, L. Brachova, B. Shanks, *Plant J.* **2008**, *54*, 536–545.
- [10] M. Selva, M. Fabris, A. Perosa, *Green Chem.* **2011**, *13*, 863–872.
- [11] A. Bomben, M. Selva, P. Tundo, L. Valli, *Ind. Eng. Chem. Res.* **1999**, *38*, 2075–2079.
- [12] a) A. Y. Platonov, A. N. Evdokimov, A. V. Kurzin, H. D. Maiygorova, *J. Chem. Eng. Data* **2002**, *47*, 1175–1176; b) M. Selva, C. A. Marques, P. Tundo, *J. Chem. Soc. Perkin Trans. 1* **1994**, 1323–1328.
- [13] a) M. Selva, P. Tundo, A. Perosa, *J. Org. Chem.* **2001**, *66*, 677–680; b) M. Selva, P. Tundo, A. Perosa, *J. Org. Chem.* **2003**, *68*, 7374–7378; c) M.

- Selva, P. Tundo, *J. Org. Chem.* **2006**, *71*, 1464–1470; d) M. Selva, A. Perosa, M. Fabris, *Green Chem.* **2008**, *10*, 1068; e) J. N. G. Stanley, M. Selva, A. F. Masters, T. Maschmeyer, A. Perosa, *Green Chem.* **2013**, *15*, 3195.
- [14] a) A. Takagaki, K. Iwatani, S. Nishimura, K. Ebitani, *Green Chem.* **2010**, *12*, 578–581; b) M. G. Álvarez, M. Plísková, A. M. Segarra, F. Medina, F. Figueras, *Appl. Catal. B* **2012**, *113–114*, 212–220; c) P. Liu, M. Derchi, E. J. M. Hensen, *Appl. Catal. A* **2013**, *467*, 124–131; d) L. Zheng, S. Xia, Z. Hou, M. Zhang, Z. Hou, *Chin. J. Catal.* **2014**, *35*, 310–331.
- [15] a) M. B. Talawar, T. M. Jyothi, P. D. Sawant, T. Raja, B. S. Rao, *Green Chem.* **2000**, *2*, 266–268; b) P. Tundo, S. Memoli, D. Hérault, K. Hill, *Green Chem.* **2004**, *6*, 609; c) G. Wu, X. Wang, B. Chen, J. Li, N. Zhao, W. Wei, Y. Sun, *Appl. Catal. A* **2007**, *329*, 106–111; d) G. D. Yadav, J. Y. Salunke, *Catal. Today* **2013**, *207*, 180–190.
- [16] M. Selva, V. Benedet, M. Fabris, *Green Chem.* **2012**, *14*, 188–200.
- [17] In this way, void spaces and preferential pathways of the reactant mixture through the catalytic bed were minimised if not ruled out; see: P. Harriot, *Chemical Reactor Design*, Marcel Dekker, New York, **2003**.
- [18] In the repeated tests performed under the same conditions, the values for the conversion and the amounts of products (determined by GC–MS) differed by less than 5% from one reaction to another.
- [19] D. Barthomeuf, *J. Phys. Chem.* **1984**, *88*, 42.
- [20] M. Selva, E. Militello, M. Fabris, *Green Chem.* **2008**, *10*, 73–79.
- [21] Y. Ono, *Cattech* **1997**, *1*, 31.
- [22] a) F. Bonino, A. Damin, S. Bordiga, M. Selva, P. Tundo, A. Zecchina, *Angew. Chem. Int. Ed.* **2005**, *44*, 4774–4777; *Angew. Chem.* **2005**, *117*, 4852–4855; b) T. Beutel, M. J. Peltre, B. L. Su, *Colloids Surf. A* **2001**, *187–188*, 319–325; c) T. Beutel, *J. Chem. Soc. Faraday Trans.* **1998**, *94*, 985–993.
- [23] P. Tundo, L. Rossi, A. Loris, *J. Org. Chem.* **2005**, *70*, 2219–2224.
- [24] a) M. Selva, S. Guidi, M. Noè, *Green Chem.* **2015**, *17*, 1008–1023; b) S. Guidi, A. Perosa, M. Noè, R. Calmanti, M. Selva, *ACS Sustainable Chem. Eng.* **2016**, *4*, 6144–6151.
- [25] a) F. Cavani, F. Trifirò, A. Vaccari, *Catal. Today* **1991**, *11*, 173–301; b) P. Bera, M. Rajamathi, M. S. Hedge, P. Vishnu Kamath, *Bull. Mater. Sci.* **2000**, *23*, 141–145; c) P. Kuśtrowski, D. Sulkowska, L. Chmielarz, A. Rafalska-Lasocha, B. Dudek, R. Dziembaj, *Microporous Mesoporous Mater.* **2005**, *78*, 11–22; d) K. J. D. MacKenzie, R. H. Meinhold, B. L. Sherriff, Z. Xu, *J. Mater. Chem.* **1993**, *3*, 1263–1269.
- [26] M. Hájek, P. Kutálek, L. Smoláková, I. Troppová, L. Capek, D. Kubicka, J. Kocík, D. N. Thanh, *Chem. Eng. J.* **2015**, *263*, 160–167.
- [27] a) Y. Ono, H. Hattori (Eds.), *Springer Series in Chemical Physics 101: Solid Base Catalysts*, Springer, Berlin, **2011**; b) S. T. Gadge, A. Mishra, A. L. Gajengi, N. V. Shahi, B. M. Bhanage, *RSC Adv.* **2014**, *4*, 50271–50276.
- [28] A. J. Parrott, R. A. Bourne, P. N. Gooden, H. S. Bevinakatti, M. Poliakov, D. J. Irvine, *Org. Process Res. Dev.* **2010**, *14*, 1420–1426.
- [29] During the purification of the final reaction mixtures, the more volatile ethers **2b/2b'** and **2e/2e'** were partly removed in the first distilled fraction of DMC or DEC.
- [30] J. S. Choi, F. S. H. Simanjuntaka, J. Y. Oh, K. I. Lee, S. D. Lee, M. Cheong, H. S. Kim, H. Lee, *J. Catal.* **2013**, *297*, 248–255.
- [31] D. J. Darensbourg, A. D. Yeung, *Green Chem.* **2014**, *16*, 247–252.
- [32] F. Leising, Z. Mouloungui, (Chryso, Institut National Polytechnique de Toulouse and Institut National de la Recherche Agronomique), US2015329468 (A1), **2015**.
- [33] a) Y. Nakao, S. Ebata, J. Chen, H. Imanaka, T. Hiyama, *Chem. Lett.* **2007**, *36*, 606–607; b) I. Franzoni, L. Guénée, C. Mazet, *Org. Biomol. Chem.* **2015**, *13*, 6338–6343.
- [34] a) Y. Liu, E. Lotero, J. G. Goodwin Jr., X. Mo, *Appl. Catal. A* **2007**, *331*, 138–148; b) H. A. Prescott, Z.-J. Li, E. Kemnitz, A. Trunschke, J. Deutsch, H. Lieske, A. Auroux, *J. Catal.* **2005**, *234*, 119–130.
- [35] A. Rodríguez, J. Canosa, A. Domínguez, J. Tojo, *Fluid Phase Equilib.* **2002**, *201*, 187–201.
- [36] J. Shen, R. D. Cortright, Y. Chen, J. A. Dumesic, *J. Phys. Chem.* **1994**, *98*, 8067–8073.
- [37] Y. Fu, H. Zhu, J. Shen, *Thermochim. Acta* **2005**, *434*, 88–92.
- [38] P. Tundo, F. Aricò, A. E. Rosamilia, S. Memoli, *Green Chem.* **2008**, *10*, 1182–1189.
- [39] J. I. Di Cosimo, V. K. Diez, M. Xu, E. Iglesia, C. R. Apesteguía, *J. Catal.* **1998**, *178*, 499–510.
- [40] B. Hallstedt, *J. Am. Ceram. Soc.* **1992**, *75*, 1497–1507.
- [41] L. Lutterotti, R. Ceccato, R. Dal Maschio, E. Pagani, *Mater. Sci. Forum* **1998**, *278–281*, 87–92. The Rietveld analysis of these samples was performed by the method proposed by Lutterotti et al. for the analysis of amorphous materials. Specifically, the pattern of an amorphous or nanocrystalline phase was fitted by using the structure of a crystalline phase with the same chemical composition. The XRD spectrum of Al₂O₃ with very broad peaks was used to obtain the pattern of the amorphous phase.
- [42] S. Vyas, R. W. Grimes, D. J. Binks, F. Rey, *Phys. Chem. Solids* **1997**, *58*, 1619–1624.
- [43] M. G. Alvarez, A. M. Segarra, S. Contrera, J. E. Sueiras, F. Medina, F. Figueras, *Chem. Eng. J.* **2010**, *161*, 340–345.
- [44] V. Vágvölgyi, S. J. Palmer, J. Kristóf, R. L. Frost, E. Horváth, *J. Colloid Interface Sci.* **2008**, *318*, 302–308.
- [45] J. C. A. A. Roelofs, J. A. van Bokhoven, A. J. van Dillen, J. W. Geus, K. P. de Jong, *Chem. Eur. J.* **2002**, *8*, 5571–5579.
- [46] a) M. León, E. Díaz, S. Ordóñez, *Catal. Today* **2011**, *164*, 436–442.
- [47] T. M. Jyothi, T. Raja, K. Sreekumar, M. B. Talawar, B. S. Rao, *J. Mol. Catal. A* **2000**, *157*, 193–198.
- [48] a) M. J. Climent, A. Corma, P. De Frutos, S. Iborra, M. Noy, A. Velty, P. Concepción, *J. Catal.* **2010**, *269*, 140–149; b) A. Navajas, G. Arzamendi, F. Romero-Sarria, M. A. Centeno, J. A. Odriozola, L. M. Gandía, *Catal. Commun.* **2012**, *17*, 189–193.
- [49] V. K. Díez, C. R. Apesteguía, J. I. Di Cosimo, *J. Catal.* **2003**, *215*, 220–233.
- [50] M. Bolognini, F. Cavani, D. Scagliarini, C. Flego, C. Perego, M. Saba, *Catal. Today* **2002**, *75*, 103–111.
- [51] The basicity data were provided by the supplier of commercial PURAL solids (SASOL). The data referred to c-HT30 and c-HT70 samples calcined at 450 °C.
- [52] a) V. Crocellà, G. Cerrato, G. Magnacca, C. Morterra, F. Cavani, L. Maselli, S. Passeri, *Dalton Trans.* **2010**, *39*, 8527–8537; b) V. Crocellà, G. Cerrato, G. Magnacca, C. Morterra, F. Cavani, S. Cocchi, S. Passeri, D. Scagliarini, C. Flego, C. Perego, *J. Catal.* **2010**, *270*, 125–135.
- [53] a) S. Abelló, F. Medina, D. Tichit, J. Perez-Ramirez, X. Rodriguez, J. E. Sueiras, P. Salagre, Y. Cesteros, *Appl. Catal. A* **2005**, *281*, 191–198; b) J. M. Fraile, N. Garcia, J. A. Mayoral, E. Pires, L. Roldan, *Appl. Catal. A* **2009**, *364*, 87–94; c) N. N. A. H. Meis, J. H. Bitter, K. P. de Jong, *Ind. Eng. Chem. Res.* **2010**, *49*, 8086–8093; d) S. Walspurger, P. D. Cobden, O. V. Safonova, Y. Wu, E. J. Anthony, *Chem. Eur. J.* **2010**, *16*, 12694–12700.
- [54] M. Selva, P. Tundo, D. Brunelli, A. Perosa, *Green Chem.* **2007**, *9*, 463.
- [55] P. G. Jessop, T. Ikariya, R. Noyori, *J. Am. Chem. Soc.* **1996**, *118*, 344.

Manuscript received: December 1, 2016

Revised: January 20, 2017

Accepted Article published: January 31, 2017

Final Article published: March 7, 2017